Biochimica et Biophysica Acta 1808 (2011) 2685–2693

Contents lists available at ScienceDirect

Biochimica et Biophysica Acta

journal homepage: www.elsevier.com/locate/bbamem

Mechanistic insights into the translocation of full length HIV-1 Tat across lipid membranes

Annegret Boll [a], Aline Jatho [a], Nadine Czudnochowski [b], Matthias Geyer [b], Claudia Steinem [a,*]

[a] Institute of Organic and Biomolecular Chemistry, Tammannstr. 2, 37077 Göttingen, Germany
[b] Max Planck Institute for Molecular Physiology, Department of Physical Biochemistry, Otto-Hahn-Str. 11, 44227 Dortmund, Germany

ARTICLE INFO

Article history:
Received 21 April 2011
Received in revised form 19 June 2011
Accepted 20 July 2011
Available online 27 July 2011

Keywords:
Arginine-rich motif
Cell penetrating peptide
Fluorescence microscopy
Giant unilamellar vesicle
Protein–membrane interaction
Transactivator of transcription

ABSTRACT

The mechanism of how full length Tat (aa 1–86) crosses artificial lipid membranes was elucidated by means of fluorescence spectroscopy and fluorescence microscopy. It was shown that full length Tat (aa 1–86) neither forms pores in large unilamellar vesicles (LUVs) nor in giant unilamellar vesicles (GUVs) composed of 1-palmitoyl-2-oleoyl-*sn*-glycero-3-phosphocholine (POPC). In contrast, an *N*-terminally truncated Tat protein (aa 35–86) that lacks the structurally defined proline- and cysteine-rich region as well as the highly conserved tryptophan residue at position 11 generates pores in artificial POPC-membranes, through which a water-soluble dye up to a size of 10 kDa can pass. By means of fluorescence microscopy, the transfer of fluorescently labeled full length Tat across POPC-bilayers was unambiguously visualized with a concomitant accumulation of the protein in the membrane interface. However, if the dye was attached to the protein, also pore formation was induced. The size of the pores was, however smaller than the protein size, *i.e.* the labeled protein with a mass of 11.6 kDa passed the membrane, while a fluorescent dye with a mass of 10 kDa was excluded from the vesicles' interior. The results demonstrate that pore formation is not the prime mechanism by which full length Tat crosses a membrane.

1. Introduction

The human immunodeficiency virus type 1 (HIV-1) Tat protein (transactivator of transcription) is a small basic protein of 86 up to 102 residues dependent on the viral isolate [1,2]. It is a key regulator of viral gene expression and stimulates transcription of viral genes about 10- to 100-fold above basal transcription levels at the stage of transcription elongation [2]. The protein is also involved in other steps of virus production and it is known to be strictly required for HIV-1 multiplication within infected cells [3]. However, the protein is not restricted to infected cells. Albeit devoid of a signal sequence, it is released by infected cells [4] and nanomolar Tat concentrations were measured in the sera of HIV-1-infected patients [5]. If the Tat protein enters non-infected cells, the replication cycle of the virus becomes more efficient after infection. Based on those effects found for extracellular Tat, it is suggested that it is involved in the progression to AIDS [1,6], and is thus considered an important target in the development of anti-HIV-1 drugs or vaccines [4,7].

To elicit cell responses, Tat needs to reach the inside of the cell, which might occur first via clathrin-mediated endocytosis [8]. It then accumulates in late endosomes, from where it has to escape to reach the cytosol and eventually localize to the nucleus. The molecular determinants that enable Tat to cross membranes as well as the membrane translocation mechanism still remain elusive.

As yet, a wealth of information has been gathered only for the HIV-1 Tat peptide, which corresponds to a 10 amino acid long basic region (aa 48–57) of the full length protein (Fig. 1). This peptide is capable of crossing plasma membranes of living cells within 3–5 min [9]. Fused to various cargo moieties, Tat peptide can even deliver fluorophores, nucleotides, proteins, drugs and genes into cells [10–16]. Its sequence comprises two lysine and six arginine residues, which makes the peptide strongly cationic (also called arginine-rich motif, ARM). From a structural and functional perspective, the Tat peptide belongs to the class of cell penetrating peptides (CPPs), which are generally composed of 10–30 amino acids containing a cluster of positively charged arginine and lysine residues. Such CPPs have been shown to cross artificial membranes and they are able to form pores [17–26]. *In vitro* studies demonstrated that pore formation also occurs during the interaction of Tat peptide with artificial membranes [27]. It has been further

Abbreviations: AF633, Alexa Fluor 633 maleimide; AF488, Alexa Fluor 488 maleimide; D3-AF488, 3 kDa dextran coupled AF488; D10-AF488, 10 kDa dextran coupled AF488; Tat-AF633, AF633 labeled full length Tat protein; ARM, arginine rich motif; CF, 5(6)-carboxyfluorescein; CPP, cell penetrating peptide; GUV, giant unilamellar vesicle; LUV, large unilamellar vesicle; PB-DMPE, pacific blue-1,2-ditetradecanoyl-*sn*-glycero-3-phosphoethanolamine, triethylammonium salt; ROI, region of interest; TR-DHPE, sulforhodamine 101 dihexadecanoylphosphatidylethanolamine; IPTG, isopropyl-β-D-1-thiogalactopyranoside; PMSF, phenylmethanesulfonylfluoride; GSH, glutathione; TEV, Tobacco etch virus; SDS-PAGE, sodium dodecylsulfate polyacrylamide gel electrophoresis

* Corresponding author at: Institute of Organic and Biomolecular Chemistry, Georg-August University, Tammannstr. 2, 37077 Göttingen, Germany. Tel.: + 49 551 39 3294; fax: +49 551 39 3228.
E-mail address: claudia.steinem@chemie.uni-goettingen.de (C. Steinem).

0005-2736/$ – see front matter © 2011 Elsevier B.V. All rights reserved.
doi:10.1016/j.bbamem.2011.07.030

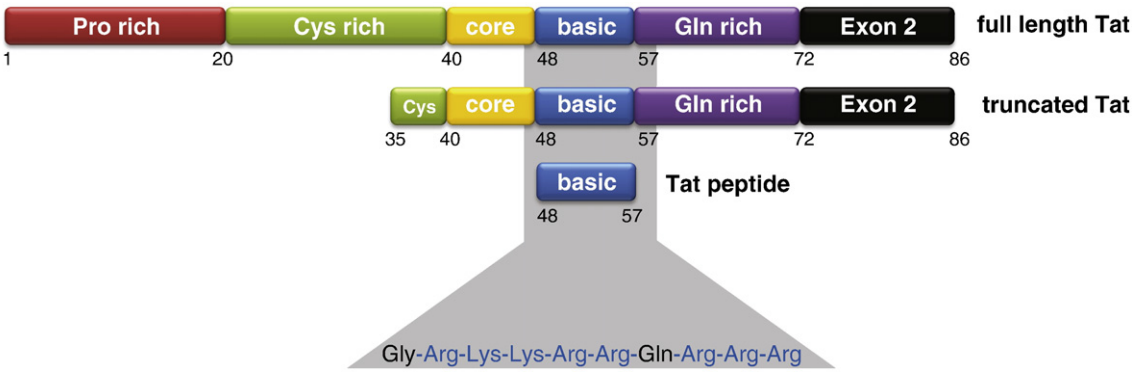

Fig. 1. Schematic drawings of the different structural regions of full length Tat and the *N*-terminally truncated protein. For comparison, the basic cluster of the Tat peptide (arginine-rich motif, ARM) is shown.

suggested that a disruption of the bilayer structure takes place resulting in the formation of inverted micelles [28]. The membrane interaction of Tat peptide is primarily driven by electrostatic forces arising from the interaction of the peptide's positive net charge with the negative charges of the phosphate groups of the lipids [29]. Non-electrostatic forces, such as hydrogen bonding and van-der-Waals forces support binding of the peptide as concluded from its binding energies [30].

Compared to the Tat peptide, much less is known about the membrane interaction of full length Tat (aa 1–86), which comprises not only the Tat peptide sequence but also several other motifs (Fig. 1). The first 21 *N*-terminal amino acids encompass an acidic and proline-rich region containing a highly conserved tryptophan residue at position 11 in HIV-1. It has been demonstrated that the Tat protein is capable of inserting into lipid monolayers and bilayers even though the overall hydrophobicity of the protein is rather low. The tryptophan residue at position 11 appears to be crucial for this insertion [31]. This stretch is followed by a cysteine-rich region (aa 22–37), a highly conserved core sequence (aa 38–47), the basic region (aa 48–57), and a glutamine-rich segment (aa 58–72) [32]. The second exon includes an RGD-motif that may mediate Tat binding to cell surface integrins [33]. The cysteine-rich region can form a zinc finger motif, and it has been demonstrated that full length Tat can form metal-linked dimers [34]. The overall structure of the protein is, however largely unfolded as deduced from CD-spectroscopy [35] and NMR-spectroscopy [36] of a reduced HIV-1 Tat (1–72) and rather flexible.

As full length Tat (aa 1–86) is structurally greatly different from Tat peptide (aa 48–57) (Fig. 1), the question needs to be answered whether the mechanism by which the protein interacts and potentially crosses a membrane is the same as that observed for the Tat peptide, *i.e.* whether it is capable of forming pores. Thus, we performed experiments with full length Tat using large unilamellar vesicles (LUVs) and giant unilamellar vesicles (GUVs) in conjunction with fluorescence spectroscopy and fluorescence microscopy. To be able to elucidate the influence of the structurally most defined region of the protein, the cysteine-rich region, we made use of an *N*-terminally truncated version of the protein lacking the first 34 amino acids (Fig. 1).

2. Materials and methods

2.1. Materials

The phospholipids POPC (1-palmitoyl-2-oleoyl-*sn*-glycero-3-phosphocholine) and Bio-cap-PE (1,2-dipalmitoyl-*sn*-glycero-3-phosphoethanolamine-*N*-cap-biotinyl, sodium salt) were purchased from Avanti Polar Lipids Inc. (Alabaster, AL, USA). TR-DHPE (sulforhodamine 101 dihexadecanoylphosphatidylethanolamine) and avidin were obtained from Sigma-Aldrich (Taufkirchen, Germany), PB-DMPE (pacific blue-1,2-ditetradecanoyl-*sn*-glycero-3-phosphoethanolamine, triethylammonium salt) Alexa Fluor 488, dextran coupled Alexa Fluor 488 and Alexa Fluor 633-C_5-maleimide were obtained from Invitrogen GmbH (Karlsruhe, Germany). The lipids were dissolved in chloroform. The water soluble dye pyranine (8-hydroxy-1,3,6-pyrenetrisulfonic acid, trisodium salt) was purchased from Acros Organics (Geel, Belgium). P-type silicon wafers (with 100 nm SiO_2, specific resistance = 1–20 Ω cm) were purchased from CrysTec (Berlin, Germany). Water was purified first through a Millipore water-purification system Milli-RO 3 plus and finally with a Millipore ultrapure water system Milli-Q plus 185 (specific resistance = 18.2 MΩ cm^{-1}) (Billerica, MA, USA).

2.2. Protein expression and purification

Genes encoding full length Tat (aa 1–86) and *N*-terminally truncated Tat (aa 35–86) were cloned into the prokaryotic expression vector pGEX-4T-1 (GE Healthcare) modified with a TEV cleavage site to generate a fusion protein with an *N*-terminal glutathione-*S*-transferase (GST) tag. Proteins were expressed and purified similarly as described [37]. Briefly, Tat proteins were expressed in *Escherichia coli* BL21(DE)3 cells (Novagen) for 4 h after induction with 0.1 mM IPTG. Cells were lysed in buffer A (20 mM Tris/HCl, 500 mM NaCl, 10% glycerol, 5 mM β-mercaptoethanol, pH 7.4) supplemented with 1 mM PMSF. The lysate was cleared by centrifugation for 30 min at 32,000 × *g* and the supernatant was applied to a GSH-Sepharose (GE Healthcare) column pre-equilibrated with buffer A. The column was washed with buffer A, followed by 10 column volumes buffer A containing 1 M NaCl. An on-column cleavage with TEV protease in buffer A was performed to cleave off the GST-tag. Tat protein was washed from the column with buffer B (50 mM Tris/HCl, 200 mM NaCl, 10% glycerol, 5 mM β-mercaptoethanol, pH 7.4), uncleaved fusion protein and GST were eluted with buffer B supplemented with 10 mM GSH. Fractions containing Tat protein were pooled and diluted in buffer C (50 mM HEPES, 10% glycerol, 5 mM β-mercaptoethanol, pH 7.5) to a final maximum salt concentration of 40 mM NaCl. The protein was further purified using a 5 mL HiTrap SP XL column (GE Healthcare). Elution of the protein was achieved with 0–1 M NaCl in buffer C using a linear gradient of 12 column volumes. Peak fractions were analyzed by SDS-PAGE. Tat containing fractions were pooled, concentrated and stored at −80 °C after flash-freezing in liquid nitrogen.

2.3. Protein labeling

Alexa Fluor 633 (AF633)-C_5-maleimide was dissolved in buffer (20 mM Tris/HCl, 100 mM NaCl, pH 7.4) to a concentration of 1 mM. 210 μL of the dye solution was added to the protein solution (800 μL, 26.4 μM full length Tat (aa 1–86) dissolved in the same buffer) and stirred at 4 °C overnight. Then, the reaction was quenched with an excess of β-mercaptoethanol. Labeled full length Tat (aa 1–86), termed Tat-AF633, was purified by FPLC (Äkta purifier UPC 10, GE

Healthcare) using a 5 mL HiTrap desalting column (GE Healthcare). The concentration of Tat-AF633 and the labeling rate was determined by UV/vis–spectroscopy at $\lambda = 280$ nm ($\varepsilon_{Tat} = 9970$ L mol^{-1} cm^{-1}), taking the absorption of free AF633 at 280 nm into account (see supplementary information, Figure S1).

2.4. Preparation of large unilamellar vesicles (LUVs)

Lipid films composed of POPC were prepared at the bottom of glass test tubes by drying the lipids dissolved in chloroform under a stream of nitrogen while heating above 30 °C followed by 3 h under vacuum. The lipid films were stored at 4 °C. Multilamellar vesicles were obtained by incubating the lipid film in 5(6)-carboxyfluorescein (CF) containing buffer (100 mM CF, 20 mM Tris/HCl, 100 mM NaCl, pH 7.4) for 30 min followed by vortexing it three times for 30 s every 5 min. The resulting multilamellar vesicles were converted into LUVs by the extrusion method using a polycarbonate membrane with a pore diameter of 1000 nm. After formation of LUVs, the external fluorescence dye was removed from the vesicles by gel filtration using a Sephadex G-25 column with NaCl containing buffer as eluent (20 mM Tris/HCl, 100 mM NaCl, pH 7.4).

2.5. Preparation of giant unilamellar vesicles (GUVs)

POPC was used for GUV formation, 1 mol% of Bio-cap-PE was added to fix the GUVs on avidin coated silicon substrates. Moreover, for fluorescence labeling, 0.1 mol% of either TR-DHPE or PB-DMPE was added. GUVs were formed by electroformation. 25 μL of the respective lipid mixture in chloroform were placed onto an indium tin oxide (ITO) coated cover slip. After removing of the solvent, the lipid film was dissolved in 300 mM sucrose in ultrapure water and GUVs were formed at 1.6 V and 12 Hz for 3 h. The successful formation of GUVs was proven by confocal laser scanning microscopy (CLSM).

2.6. Release experiments

The release of 5(6)-carboxyfluorescein (CF) from LUVs composed of POPC was monitored by the time dependent increase in fluorescence intensity of CF after addition of full length Tat (aa 1–86) and *N*-terminally truncated Tat (aa 35–86). Fluorescence emission of CF was measured at $\lambda_{em} = 520$ nm, while it was excited at $\lambda_{ex} = 490$ nm. To determine the maximum fluorescence intensity F_0, the LUVs were destroyed by adding 2 μL of the detergent Triton X-100 (10% (*w*/*v*)) to a total volume of 800 μL. All experiments were performed using the fluorometer FP6500 (Jasco, Gotha, Germany).

2.7. GUV based assays

First, the silicon substrates were cleaned with isopropanol and ultrapure water. Then, the silicon substrates were incubated in an aqueous solution of NH_3/H_2O_2 ($H_2O/NH_3/H_2O_2$, 5:1:1) for 15 min at 70 °C. The cleaned substrates were rinsed with ultrapure water and mounted in an open Teflon chamber. For avidin coating, they were incubated for 1 h with 200 μL of a 50 nM avidin solution in buffer (20 mM Tris/HCl, 100 mM NaCl, pH 7.4). Finally, the substrates were rinsed with buffer.

For the *pore formation assay*, 100 μL of the GUV suspension, which were filled with 300 mM sucrose, were dissolved in buffer solution containing 0.5 μM full length Tat (aa 1–86) or the *N*-terminal truncated Tat (aa 35–86). The solution was added to the avidin coated silicon substrate, where the GUVs were allowed to bind via biotin to the avidin monolayer for about 10 min.

For the *translocation assay*, 20 μL of the GUV suspension were dissolved in buffer solution containing 0.5 μM full length Tat-AF633. The solution was again added to an avidin coated silicon substrate to bind the GUVs onto the substrate. Fluorescence images of the GUVs were obtained in a time resolved manner. The same experiments were performed in the presence of the water soluble dyes Alexa Fluor 488 (AF488), 3 kDa dextran coupled Alexa Fluor 488 (D3-AF488) and 10 kDa dextran coupled Alexa Fluor 488 (D10-AF488).

2.8. Confocal laser scanning microscopy

Fixed GUVs were visualized with an upright confocal laser scanning microscope (LSM 710, Carl Zeiss AG, Jena, Germany) with a water immersion objective W Plan-Apochromat 63×/1,0 VIS-IR. The fluorescent dyes TR-DHPE and PB-DMPE were excited at $\lambda = 594$ nm, and $\lambda = 405$ nm, respectively. The water soluble dyes pyranine, Alexa Fluor 488 and the dextran coupled Alexa Fluor 488 were excited at $\lambda = 488$ nm and Tat-AF633 at $\lambda = 633$ nm. Fluorescence image analysis was performed using the ZEN software (Carl Zeiss AG, Jena, Germany).

3. Results

Previously, it has been shown that the cell penetrating HIV-1 Tat peptide comprising amino acids 48–57 is capable of forming pores in lipid bilayers of giant unilamellar vesicles (GUVs) dependent on the lipid composition [38,39], while there was no pore formation observed in large unilamellar vesicles (LUVs) [30,40–42]. Pore formation or disruption of the bilayer structure can provide a pathway for the highly charged peptide to cross lipid membranes, which might be influenced by the membrane curvature. Thus, we first addressed the question whether the native full length Tat protein (aa 1–86) can form pores in LUVs and GUVs, respectively. Besides the full length protein, we used an *N*-terminally truncated protein (aa 35–86), which lacks the proline- and cysteine-rich regions that are structurally most defined [43], but still harbors the arginine rich motif (basic cluster) (Fig. 1). CD-spectra reveal no significant structural differences between full length Tat and the truncated version of the protein. Both proteins adopt a predominant random coil conformation in solution as reported previously (see supplementary information, Figure S2) [35,36].

3.1. Pore formation induced by Tat proteins in LUVs

The release of 5(6)-carboxyfluorescein (CF) from LUVs is a well known method to investigate pore formation processes in lipid bilayers by water soluble peptides or proteins [44,45]. The method is based on the self-quenching of CF at high concentrations ($c > 50$ mM) entrapped in the inner volume of the vesicles. When a protein or peptide perturbs the bilayer integrity, CF is released, which leads to an increase in fluorescence intensity as a result of its dilution. Here, the relative fluorescence intensity was measured in a time dependent manner. First, the fluorescence intensity of the CF-filled POPC LUVs was monitored prior to the addition of the protein. Then, 0.5 μM of full length Tat (aa 1–86) or truncated Tat (aa 35–86) was added and the CF fluorescence intensity was monitored *vs.* time ($F(t)$). Even at a lipid-to-protein ratio of only 3:1 the full length Tat protein (aa 1–86) did not cause any CF release from the lipid vesicles (Fig. 2). In contrast, the truncated version of the Tat protein (aa 35–86) leads to a minute CF release of about 2%. This indicates that there is a small propensity of the *N*-terminally truncated version of the Tat protein to form pores, through which the water soluble dye CF can pass, while there is no pore formation observable in LUVs in the presence of full length Tat.

3.2. Pore formation induced by Tat proteins in GUVs

Giant unilamellar vesicles (GUVs) have the advantage that each individual vesicle can be inspected by confocal laser scanning microscopy. They were doped with the membrane-embedded dye TR-DHPE and immobilized via a membrane-confined biotin anchor to

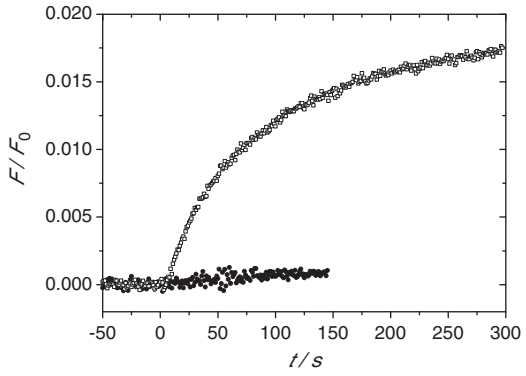

Fig. 2. Release of 5(6)-carboxyfluorescein from POPC vesicles as a function of time after the addition of full length Tat (aa 1–86) (closed symbols) and *N*-terminally truncated Tat (aa 35–86) (open symbols).

an avidin coated silicon substrate (Fig. 3A) to be able to visualize the POPC GUVs by an upright fluorescence microscope. To investigate whether the Tat proteins are capable of generating pores, through which a water soluble dye can pass, GUVs were placed in buffer (20 mM Tris/HCl, 100 mM NaCl, pH 7.4) containing 200 μM of the water-soluble fluorescent dye pyranine and 0.5 μM full length Tat (aa 1–86) or *N*-terminally truncated Tat (aa 35–86). After 2 h of incubation, the fluorescence intensity of the dye inside the GUVs was determined using a region of interest (ROI) and normalized to that outside of the vesicles, which is termed F_{rel} (Fig. 3A). After 2 h, a distribution of the fluorescence intensity inside the vesicles was read out (see supplementary information, Figure S3). To obtain a value that reflects whether the vesicles are predominantly filled with the dye or not, a threshold value of $F_{rel}>0.5$ was chosen, *i.e.* a GUV was regarded as dye-filled if $F_{rel}>0.5$. As a control, GUVs were incubated in the dye solution without the addition of Tat protein and F_{rel} was read out after 2 h. For statistical analysis, at least three independent experiments were performed. For the blank sample without Tat, 15% of the GUVs were filled with the fluorescent dye pyranine after 2 h. After incubation with full length Tat (aa 1–86), 24% of the POPC GUVs were filled with the dye (Fig. 3B) indicating that the majority of the GUVs remain intact and no significant pore formation is observed. This is in contrast to the results obtained for Tat peptide (aa 48–57), which has been shown to form physical pores in neutral GUV membranes (DOPC/DPPC/Chol, 4:2:2) under buffer conditions [39]. It is conceivable that pore formation is determined by the length of the peptide. Already from the dye release experiments on LUVs (Fig. 2) one can conclude that the *N*-terminally truncated Tat protein shows a greater tendency to form pores. Thus, the same experiments on POPC GUVs were performed, but full length Tat was replaced by the truncated protein. Indeed, we found an increased entry of pyranine of 59% compared to only 24% for full length Tat (Fig. 3B). Interestingly, even though the truncated protein is much longer (51 amino acids) than the Tat peptide (10 amino acids), it behaves more similarly to the Tat peptide than to the Tat protein (86 amino acids).

As the results demonstrate that the *N*-terminally truncated version of Tat induces pores in GUV membranes, we next elucidated the size of the pores that are formed by using fluorophores that are attached to dextran molecules of different sizes. We used AlexaFluor488 attached either to a 3 kDa large dextran (D3-AF488) or to a 10 kDa large dextran (D10-AF488). POPC GUVs were incubated with 0.5 μM truncated Tat (aa 35–86) in D3-AF488 and D10-AF488 containing buffer and F_{rel} was determined (Fig. 3C) after 2 h. In the case of D3-AF488, more than 70% of the POPC GUVs were filled with the dye. Even in the presence of D10-AF488, 50% of the GUVs were still filled with the fluorophore. These results demonstrate that the truncated protein forms pores, which are large enough that a molecule of 10 kDa can pass and they imply that it is possible for the truncated Tat protein

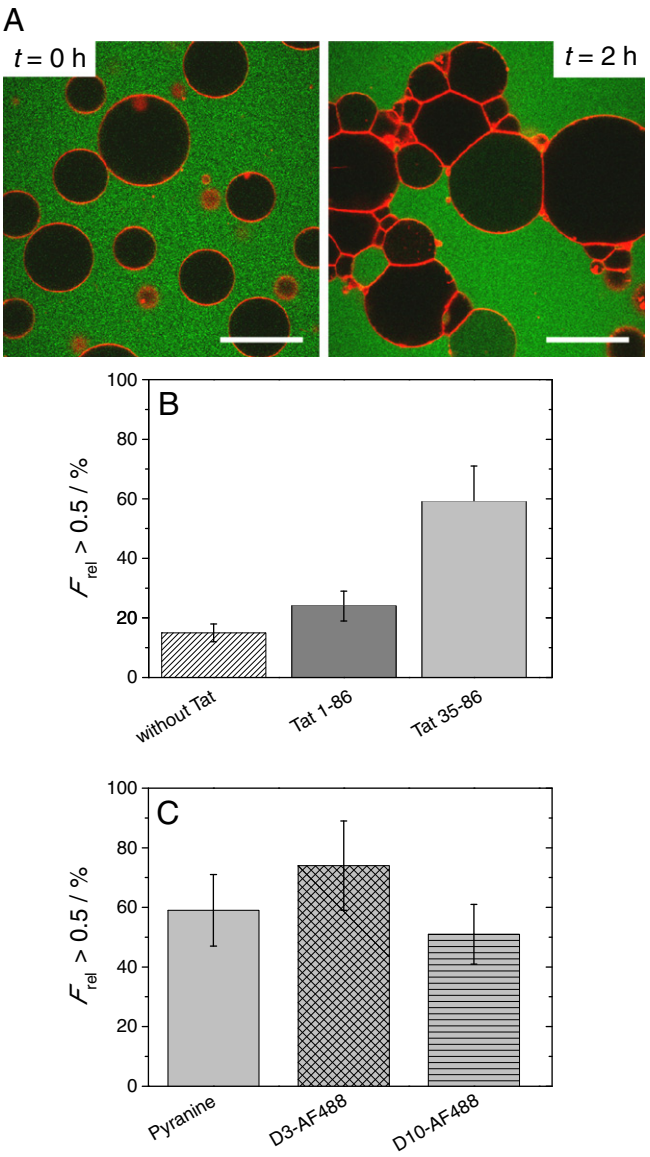

Fig. 3. A. Fluorescence images of POPC GUVs before ($t=0$ h) and after 2 h of incubation with 0.5 μM full length Tat (aa 1–86). While most of the GUVs appear black inside, very few are filled with the dye pyranine. Green: pyranine, red: TR-DHPE. Scale bars: 50 μm. B. Fraction of filled POPC GUVs ($F_{rel}>0.5$). GUVs were incubated for 2 h without protein ($n=286$), with 0.5 μM full length Tat (aa 1–86) ($n=812$) and with 0.5 μM of *N*-terminally truncated Tat (aa 35–86) ($n=284$) in pyranine containing buffer (20 mM Tris/HCl, 100 mM NaCl, 200 μM pyranine, pH 7.4). C. Fraction of filled POPC GUVs ($F_{rel}>0.5$). GUVs were incubated for 2 h with 0.5 μM *N*-terminally truncated Tat (aa 35–86) in pyranine containing buffer ($n=284$) (20 mM Tris/HCl, 100 mM NaCl, 200 μM pyranine, pH 7.4), D3-AF488 containing buffer ($n=138$) (20 mM Tris/HCl, 100 mM NaCl, 50 nM D3-AF488, pH 7.4) and D10-AF488 containing buffer ($n=165$) (20 mM Tris/HCl, 100 mM NaCl, 50 nM D10-AF488, pH 7.4).

with a molecular mass of 6.2 kDa to pass the membrane via such pores.

3.3. Translocation of fluorescently labeled full length Tat

In contrast to the *N*-terminally truncated Tat protein, the full length protein does not significantly form pores in lipid bilayers at a concentration of 0.5 μM. Thus, we next investigated, whether the protein is able to translocate across the lipid bilayer even without forming pores. To allow for the detection of the protein position, Tat was labeled with an AlexaFluor 633 fluorescence dye (Tat-AF633). POPC GUVs were added to a 0.5 μM solution of the labeled protein and

fluorescence images were taken every 15 s to localize the protein via its fluorescence in a time resolved manner (Fig. 4). The relative fluorescence intensity was read out using two ROIs as shown in Fig. 4A, which is plotted as a function of time as depicted in Fig. 4B. Interestingly, no protein translocation was observed within a rather long period of time ranging from 1 to 1.5 h. However, after that delay time, a very fast change in fluorescence intensity within the GUV is detected and the fluorescence intensity increases rapidly to the value outside the vesicle ($F_{rel}=1$). From 18 independent measurements with Tat-AF633 in a concentration range of 0.1 μM to 1.0 μM, we were able to determine a rate constant of $k=(0.017\pm0.007)\,s^{-1}$ for the translocation process by fitting an exponential function to the data (Fig. 4B). Within the concentration range analyzed, we did not observe any dependency in the translocation kinetics on the Tat protein concentration. As the assay relies on the fluorescence intensity of the Tat protein, a concentration lower than 0.1 μM could not be used owing to the limitation of fluorescence detection. We refrained from using concentrations larger than 1 μM to be consistent with most other studies on Tat peptide [46–48] and the release experiments.

Of note, translocation of full length Tat-AF633 was observed concomitantly with an increased fluorescence intensity of the fluorophore at the membrane interface (Fig. 4C). Fig. 4D displays a characteristic relative fluorescence intensity profile along the white line shown in Fig. 4C. The increased fluorescence intensity of Tat-AF633 at the GUV membrane was normalized to the fluorescence intensity of Tat-AF633 in the environment of the GUVs revealing an increase in fluorescence intensity in the plane of the membrane by almost 40%.

From the observation that the fluorescently labeled protein Tat-AF633 is found in the GUV lumen after 2 h, while a water-soluble dye is excluded from the GUV interior if incubated with unlabeled full length Tat (aa 1–86), one could conclude that the protein crosses the membrane without pore formation. However, in the two sets of experiments, two different proteins were used: unlabeled protein was used for the elucidation of pore formation, while labeled protein was used for the translocation assay. It is conceivable that the labeling alters the behavior of the protein. Thus, the translocation assay was repeated with fluorescently labeled full length Tat (Tat-AF633) in the presence of a water-soluble dye to investigate possible pore formation (Fig. 5A). As water-soluble dye, AlexaFluor 488 was used to prevent a crosstalk between this dye and Tat-AF633. Again, POPC GUVs were placed in buffer containing the water-soluble dye AlexaFluor 488 and the GUVs were incubated with 0.5 μM Tat-AF633. After 2 h, the fluorescence intensity of the water-soluble dye inside the GUVs was determined using a region of interest (ROI) and normalized to that outside of the vesicles. Without additional water-soluble dye, 56% of the GUVs were found to contain Tat-AF633 (Tat-AF633, Fig. 5B I). In the absence of the protein (free AF633, Fig. 5B II) the free dye AF633 was found in only 10% of the GUVs. However, in contrast to the results with non-labeled full length Tat, the number of GUVs that are filled with the water-soluble dye AF488 (AF488, Fig. 5B III) after 2 h of

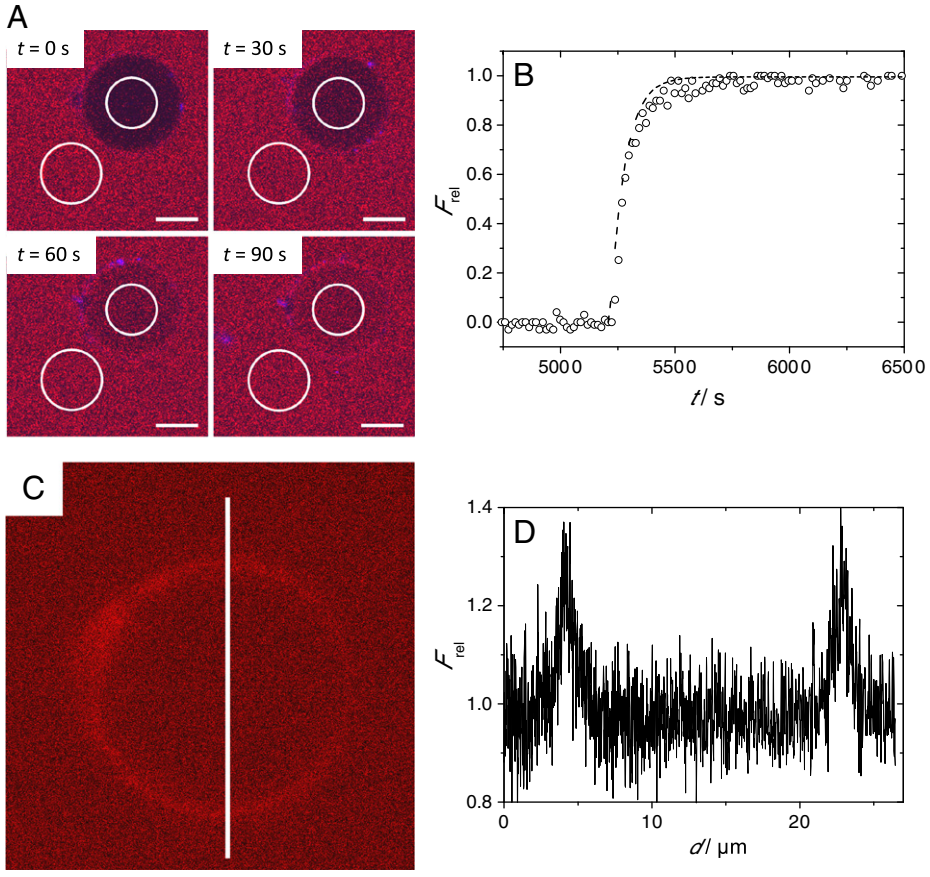

Fig. 4. A. Fluorescence images of a POPC GUV before (set to $t=0$ s) and during the process of Tat-AF633 translocation ($t=30$, 60, and 90 s). 0.5 μM of Tat-AF633 was added to POPC GUVs in 20 mM Tris/HCl, 100 mM NaCl, pH 7.4. The white circles show the ROIs. Scale bars: 5 μm. B. Time course of the relative fluorescence intensity F_{rel} within a ROI positioned in the POPC GUV during incubation with 0.5 μM full length Tat-AF633. The protein was added at $t=0$ s. An increase in F_{rel} was observed after a delay time of 5200 s. The dashed line is a result of fitting $F_{rel}=F_{rel,max}(1-\exp\{-k(t-t_0)\})$ to the data with $k=0.014\,s^{-1}$. C. Fluorescence image of a POPC GUV after 2 h incubation with 0.5 μM full length Tat-AF633 in 20 mM Tris/HCl, 100 mM NaCl, pH 7.4. As Tat-AF633 has passed the membrane, the fluorescence intensity inside and outside the GUV is equal. D. Relative intensity profile along the white line (length: 27 μm) shown in C, demonstrating the increased fluorescence intensity in the membrane region. $F_{membrane}/F_{environment}$ is the relative fluorescence intensity of Tat-AF633 in the membrane region, normalized to the fluorescence intensity of Tat-AF633 outside the GUV. The values are calculated by using profile lines (average of 100 lines) using ImageJ.

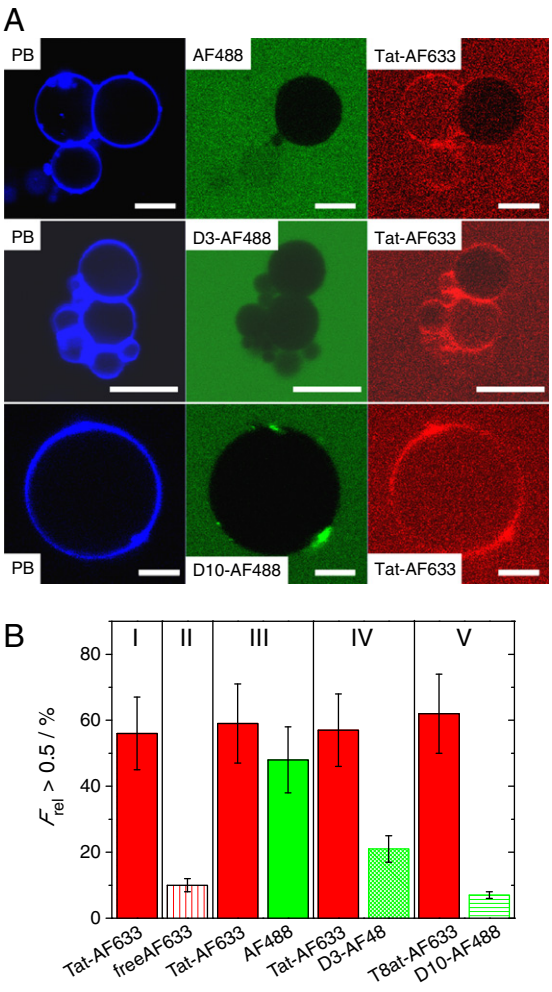

Fig. 5. A. Fluorescence images of PB-DMPE doped POPC GUVs (blue) incubated with Tat-AF633 (red) in AF488 containing buffer (green) (20 mM Tris/HCl, 100 mM NaCl, 20 nM AF488, pH 7.4), D3-AF488 containing buffer (green) (20 mM Tris/HCl, 100 mM NaCl, 50 nM D3-AF488, pH 7.4) and D10-AF488 containing buffer (green) (20 mM Tris/HCl, 100 mM NaCl, 50 nM D10-AF488, pH 7.4). Scale bars: 10 μm (AF488), 10 μm (D3-AF488) and 5 μm (D10-AF488). B. Fraction of POPC GUVs with F_{rel}>0.5 after 2 h of incubation with 0.5 μM Tat-AF633 as a function of water soluble dye containing buffer. Shown are the results for the blank sample of POPC GUVs incubated in AF633 containing buffer (n=217) (20 mM Tris/HCl, 100 mM NaCl, 14 μM AF633, pH 7.4), POPC GUVs incubated with Tat-AF633 in NaCl containing buffer (n=309) (20 mM Tris/HCl, 100 mM NaCl, pH 7.4), POPC GUVs incubated with Tat-AF633 in AF488 containing buffer (n=126) (20 mM Tris/HCl, 100 mM NaCl, 20 nM AF488, pH 7.4), POPC GUVs incubated with Tat-AF633 in D3-AF488 containing buffer (n=182) (20 mM Tris/HCl, 100 mM NaCl, 50 nM D3-AF488, pH 7.4) and POPC GUVs incubated with Tat-AF633 in D10-AF488 containing buffer (n=93) (20 mM Tris/HCl, 100 mM NaCl, 50 nM D10-AF488, pH 7.4).

incubation with 0.5 μM Tat-AF633 is twice as high (48%, for comparison see Fig. 3B). The number of Tat-AF633 filled GUVs remains the same (Tat-AF633, Fig. 5B III). This result implies that the attached fluorophore apparently changes the behavior of the protein, *i.e.* the interaction of the protein with the membrane results in pores through which the 0.7 kDa large water-soluble dye can pass. To elucidate the pore formation in more detail, we again made use of fluorophores attached to dextrans of different sizes. Incubation of POPC GUVs with 0.5 μM Tat-AF633 in the presence of D3-AF488 containing buffer leads to only 21% of the GUVs that contained the water-soluble dye D3-AF488, while again more than 50% of the GUVs were filled with Tat-AF633 (Fig. 5B IV). If the size of the dextran was increased to 10 kDa, only very few GUVs (7%) were found to be filled with the dye, while again about 60% of the GUVs were filled with Tat-AF633 (Fig. 5B V).

These results indicate that labeled Tat-AF633 does form pores in membranes but the pores are rather small. The fact that the dye transfer of the 3 kDa large dextran molecule is already strongly hindered compared to the neat AF488 dye suggests that the pores are much smaller than the size of full length Tat with a mass of 10.3 kDa (11.6 kDa for full length Tat-AF633). This is in contrast to the *N*-terminally truncated Tat, where the 10 kDa dextran molecule passes the membrane to the same extent as the free dye, which demonstrates that the truncated Tat protein forms significantly larger pores (Fig. 3C).

We asked the question whether the translocation of the protein occurs simultaneously with the dye transfer or whether translocation can be observed without the transfer of intermediate sized dextran-coupled fluorophore. To analyze this, fluorescence images of Tat-AF633 and POPC GUVs in D3-AF488 containing buffer were taken in a time dependent manner. At t=0 h, POPC GUVs are neither filled with D3-AF488 (green) nor with Tat-AF633 (red). After 1 h, Tat-AF633 started to translocate across the membrane into the POPC GUV lumen indicated by the increasing fluorescence intensity of Tat-AF633 inside the GUV. However, D3-AF488 still remains outside the GUV. After 2 h, the Tat concentration inside equals that outside, while the fluorophore D3-AF488 still remains outside. This demonstrates that not the translocation of the 11.6 kDa protein itself leads to the entry of the 3 kDa large water-soluble dye in the GUVs. The very small dye AF488 with a mass of 0.7 kDa, however translocates simultaneously with the protein suggesting that small perturbations within the membrane occur while the protein passes the membrane.

4. Discussion

Our results suggest that native full length Tat (aa 1–86) does not form pores in unilamellar POPC vesicles under physiological buffer conditions. We found neither a dye release from LUVs, even at very large protein concentrations, nor a dye entry into GUVs induced by full length Tat. In contrast, the *N*-terminally truncated Tat protein (aa 35–85) that lacks the proline-rich and cysteine-rich region is capable of forming pores in POPC LUVs and POPC GUVs. However, pore formation in POPC LUVs induced by truncated Tat was only minute. It was more significant in GUVs with pore sizes that allowed a 10 kDa sized dextran to enter the vesicle interior. This implies that also the *N*-terminally truncated protein with a mass of 6.2 kDa can in principle pass the membrane via induced pores.

This is different from the results obtained by the group of Kubitscheck [39]. They have shown that micromolar concentrations of Tat peptide form 1–2 nm large pores in GUVs (containing phosphatidylethanolamine, PE, or phosphatidylserine, PS) through which 3 kDa large dyes can pass but not 10 kDa large ones. These results were obtained in the absence of ions and no pore formation was observed in neutral phosphatidylcholine (PC) membranes. In PBS buffer, the situation was quite different. Here, the group reported [39] that Tat peptide translocation occurs even through neutral lipid membranes (DOPC/DPPC/Chol, 4:4:2) with a concomitant efflux of the water soluble dye Alexa488 demonstrating that very small pores are formed by the Tat peptide in the presence of ions. The results suggest that the mechanism of Tat peptide translocation might be associated with its pore formation capability, which is supported by molecular dynamics simulations. Herce and Garcia [27] demonstrated that the Tat peptide interacts with the phosphate head groups of the lipid bilayer on both sides, resulting in an insertion of the charged side chains of the peptide, thus nucleating the formation of a transient pore, followed by the translocation of the Tat peptide. Further evidence into this direction is given by Mishra et al. [38], who found that the Tat peptide induced a saddle-splay curvature in PC/PE/PS (2:2:1) membranes of a GUV resulting in pores through which the peptide could enter the interior. In contrast, pore formation induced by the Tat peptide was not observed in LUV membranes composed of

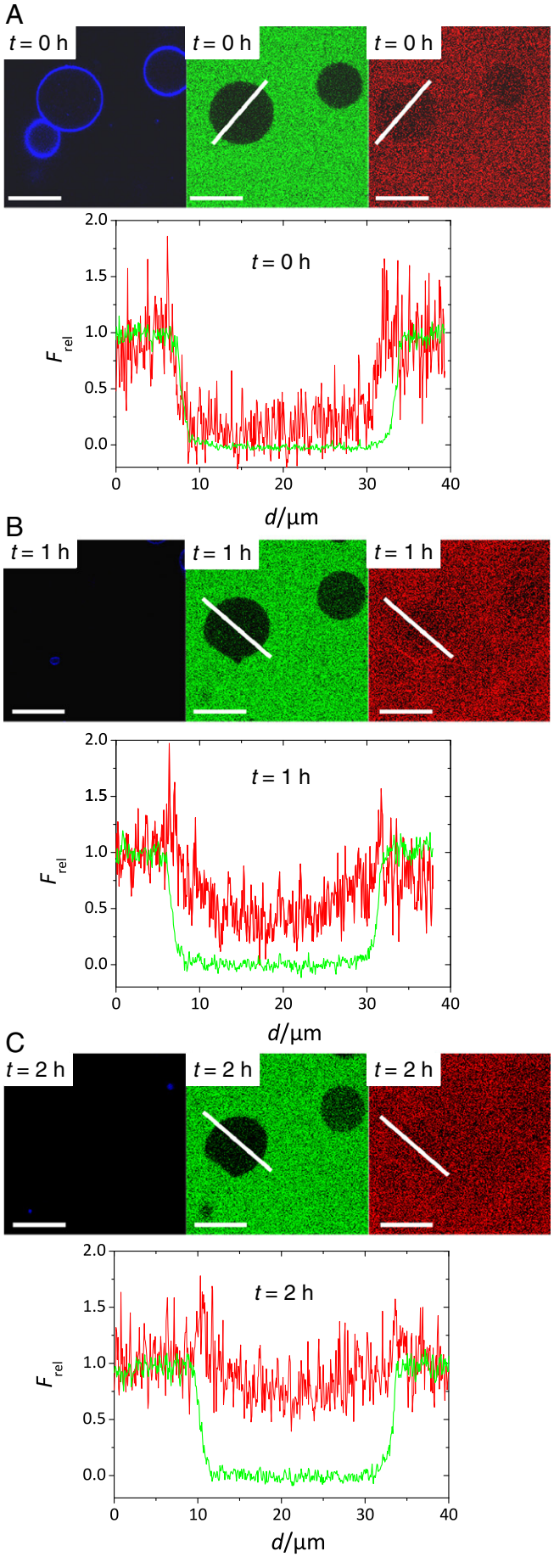

DOPC/DOPG (6:4) down to a lipid-to-peptide ratio of 17:1 under physiological conditions. Translocation of the Tat peptide into LUVs in the presence of ions was also not found, neither in neutral PC-membranes nor in negatively charged PC/PG-membranes [40,49]. These findings point in the direction that membrane curvature might play a central role in pore formation.

Pore formation cannot be attributed only to the basic Tat peptide (aa 48–57). As we observed no pore formation in GUV and LUV POPC membranes for the full length protein under buffer conditions but for the *N*-terminally truncated protein, other structural contributions appear to be decisive, as both proteins contain the ARM. One major difference between full length and truncated protein is the *N*-terminus (aa 1–34). The *N*-terminus is a structurally ordered region as deduced from the crystal structure of the protein in complex with human P-TEFb [43]. In the absence of a stabilizing co-factor, the proline-rich region of Tat is supposed to be rather flexible and folded as a random coil [36,50], whereas the cysteine-rich region might adopt a more compact fold by the formation of one or two zinc finger motifs [43]. The *N*-terminus also contains a conserved tryptophan residue at position 11, by which Tat has been shown to be able to insert into lipid membranes [31]. It is conceivable that the ordered structure in conjunction with the tryptophan residue orients the inserted protein in neutral lipid bilayers, which thus prevents pore formation. The truncated Tat protein (aa 35–86) as well as the Tat peptide are more flexible and lack the tryptophan residue, which might result in a less ordered structure in neutral lipid bilayers, so that pore formation is favored in the presence of buffer. It has been shown that even though the arginine-rich motif appears to be folded, it is structurally very flexible. When bound to TAR, it adopts an α-helical fold in full length Tat [51], but an anti-parallel β-strand like structure was determined for a short peptide, which corresponds to the Tat cell penetrating peptide [51–53]. These different conformations depending on the molecular co-factors indicate the flexibility and dynamics of the Tat translocation sequence. Another aspect to be considered might be the overall charge density at physiological pH, which is lowest for full length Tat (aa 1–86) (p*I* = 9.7) followed by the *N*-terminally truncated protein (aa 35–86) (p*I* = 11.3) and largest for the cell penetrating Tat peptide (aa 48–57) (p*I* = 12.7). A higher charge density might also facilitate pore formation. This is however, not reflected in the size of the pores. Pore sizes reported by Ciobanasu et al. [39] are a little smaller than the sizes we found for truncated Tat protein (aa 35–86). There was no or only a certain efflux of the 3 kDa dextran coupled dye, while we found that a 10 kDa dextran coupled dye could pass the membrane when the GUVs are incubated with truncated Tat (aa 35–86).

Fluorescence labeling of full length Tat (Tat-AF633) enabled us to investigate whether this protein is able to cross lipid membranes. Interestingly, Tat-AF633 is capable of translocating across POPC GUV membranes. In contrast to the non-labeled full length protein, it forms small pores, through which the water-soluble dye AF488 can pass. However, the pores themselves are not large enough for a 10 kDa dextran molecule to access the inner compartment of the vesicle, which suggests that the labeled protein with a molecular mass of 11.6 kDa does not cross the membrane via these pores. This finding is supported by the observation that the labeled protein passes the POPC membrane of a GUV without a transfer of the 3 kDa large dextran molecule (Fig. 6).

Fig. 6. Fluorescence images of PB-DMPE doped POPC GUVs with Tat-AF633 (red) in D3-AF488 containing buffer (green) (20 mM Tris/HCl, 100 mM NaCl, 50 nM D3-AF488, pH 7.4) at A. *t* = 0 h, B. *t* = 1 h and C. *t* = 2 h. Scale bars: 20 µm. The relative intensity profiles along the white lines show the fluorescence intensities of D3-AF488 (green) and Tat-AF633 (red), each normalized to the fluorescence intensity outside the GUV.

Prior to its translocation, the protein accumulates in the GUV membrane. Such accumulation will probably disturb the integrity of the membrane, which might favor small pores to be formed. Moreover, such accumulation might explain why there is no concentration dependence of Tat entry in the vesicle in a concentration range of 0.1–1.0 μM. It is assumed that the protein concentration within the membrane and not outside the membrane is decisive for the translocation to occur. Curnow et al. [47] also found that labeled Tat peptide accumulates in the membrane of 5 μm sized DOPC vesicles. The assumption that the protein requires a certain local concentration in the membrane of the GUV to pass the bilayer would explain why there is a delay between protein addition and translocation. It is conceivable that Tat forms oligomers in the membrane, as observed by Tosi et al. [54], which leads to the observed accumulation and eventually to the protein transfer. Further evidence for an insertion of the protein in lipid bilayers is given by Yezid et al. [31], who demonstrated that full length Tat inserts into lipid monolayers and vesicles at pH 6.0. They attributed the insertion of Tat to the highly conserved tryptophan residue in position 11, which is not present in truncated Tat (aa 35–86) or the Tat peptide (aa 48–57) and might explain why the shorter Tat versions behave differently compared to the full length protein.

In several studies, fluorescently labeled Tat peptide was used to investigate its interaction with lipid model membranes [38–40,46,47]. Of note, our experiments demonstrate that native full length Tat behaves differently than fluorescently labeled full length Tat. Only the fluorescently labeled version generates small pores in GUV membranes. This indicates that the fluorescent dye might influence the protein structure and thus its interaction with the membrane.

5. Conclusions

The translocation of full length Tat has been investigated by means of fluorescence spectroscopy and fluorescence microscopy leading to the conclusion that the protein does not form pores in LUVs and GUVs, while a truncated version of the protein lacking the ordered proline- and cysteine-rich region forming a zinc finger motif is able to form pores in neutral membranes. This result lets us conclude that not only the basic cluster referred to as the Tat cell penetration peptide determines whether pores are formed but rather the overall charge density of the protein and its global flexibility. Full length Tat is capable of translocating across a neutral GUV membrane under physiological conditions. However, the attached fluorescent dye alters the interaction of the protein with the membrane. It results in a disturbance of the lipid bilayer so that small molecules can enter the vesicle interior. In contrast, molecules of a size similar to that of the protein itself do not enter the vesicle's lumen. These results illustrate that the translocation mechanism is not directly dependent on the pore formation process but presumably relies on an accumulation of the protein in the membrane, which produces a disturbance of the membrane structure to let the protein through.

Acknowledgment

We thank Natascha Dietrich for the release experiments. N.C. was supported by a grant from the Fond der Chemischen Industrie (FCI). This work was supported by a grant from the Deutsche Forschungsgemeinschaft to M.G. (GE-976/5).

Appendix A. Supplementary data

Supplementary data to this article can be found online at doi:10.1016/j.bbamem.2011.07.030.

References

[1] M.C.D.G. Huigen, W. Kamp, H.S.L.M. Nottet, Multiple effects of HIV-1 *trans*-activator protein on the pathogenesis of HIV-1 infection, Eur. J. Clin. Invest. 34 (2004) 57–66.
[2] K.A. Jones, B.M. Peterlin, Control of RNA initiation and elongation at the HIV-1 promotor, Annu. Rev. Biochem. 63 (1994) 717–743.
[3] K. Strebel, Virus-host interactions: role of HIV proteins Vif, Tat and Rev, AIDS 17 (2003) 25–34.
[4] B. Ensoli, G. Barillari, S.Z. Salahuddin, R.C. Gallo, F. Wong-Staal, Tat protein of HIV-1 stimulates growth of cells derived from Kaposi's sarcoma lesions of AIDS patients, Nature 345 (1990) 84–86.
[5] H. Xiao, C. Neuveut, H.L. Tiffany, M. Benkirane, E.A. Rich, P.M. Murphy, K.T. Jeang, Selective CXCR4 antagonism by Tat: implications for in vivo expansion of coreceptor use by HIV-1, Proc. Natl. Acad. Sci. USA 97 (2000) 11466–11471.
[6] J.E. King, E.A. Eugenin, C.M. Buckner, J.W. Berman, HIV tat and neurotoxicity, Microbes Infect. 8 (2006) 1347–1357.
[7] S. Hwang, N. Tamilarasu, K. Kibler, H. Cao, A. Ali, Y.H. Ping, K.T. Jeang, T.M. Rana, Discovery of a small molecule Tat-trans-activation-responsive RNA antagonist that potently inhibits human immunodeficiency virus-1 replication, J. Biol. Chem. 278 (2003) 39092–39103.
[8] A. Vendeville, F. Rayne, A. Bonhoure, N. Bettache, P. Montcourrier, B. Beaumelle, HIV-1 Tat enters T cells using coated pits before translocating from acidified endosomes and eliciting biological responses, Mol. Biol. Cell 15 (2004) 2347–2360.
[9] G. Tunnemann, R.M. Martin, S. Haupt, C. Patsch, F. Edenhofer, M.C. Cardoso, Cargo-dependent mode of uptake and bioavailability of TAT-containing proteins and peptides in living cells, FASEB J. 20 (2006) 1775–1784.
[10] R. Fischer, M. Fotin-Mleczek, H. Hufnagel, R. Brock, Break on through to the other side-biophysics and cell biology shed light on cell-penetrating peptides, ChemBioChem 6 (2005) 2126–2142.
[11] M.C. Morris, S. Deshayes, F. Heitz, G. Divita, Cell-penetrating peptides: from molecular mechanisms to therapeutics, Biol. Cell 100 (2008) 201–217.
[12] V.P. Torchilin, Cell penetrating peptide-modified pharmaceutical nanocarriers for intracellular drug and gene delivery, Biopolymers 90 (2008) 604–610.
[13] F. Heitz, M.C. Morris, G. Divita, Twenty years of cell-penetrating peptides: from molecular mechanisms to therapeutics, Br. J. Pharmacol. 157 (2009) 195–206.
[14] P. Lundberg, Ü. Langel, A brief introduction to cell-penetrating peptides, J. Mol. Recognit. 16 (2003) 227–233.
[15] V. Sebbage, Cell-penetrating peptides and their therapeutic applications, Biosci. Horiz. 2 (2009) 64–72.
[16] J. Howl, I.D. Nicholl, S. Jones, Cell-penetrating peptides. The many futures for cell-penetrating peptides: how soon is now? Biochem. Soc. Trans. 35 (2007) 767–769.
[17] P.E.G. Thoren, D. Persson, M. Karlsson, B. Norden, The Antennapedia peptide penetratin translocates across lipid bilayers — the first direct observation, FEBS Lett. 482 (2000) 265–268.
[18] H. Binder, G. Lindblom, Charge-dependent translocation of the Trojan peptide penetratin across lipid membranes, Biophys. J. 85 (2003) 982–995.
[19] K.V.R. Reddy, R.D. Yedery, C. Aranha, Antimicrobial peptides: premises and promises, Int. J. Antimicrob. Agents 24 (2004) 536–547.
[20] Y. Tamba, M. Yamazaki, Magainin 2 induced pore formation in the lipid membrane depends on its concentration in the membrane interface, J. Phys. Chem. 113 (2009) 4846–4852.
[21] Y. Tamba, M. Yamazaki, Single giant unilamellar vesicle method reveals effect of antimicrobial peptide magainin 2 on membrane permeability, Biochemistry 44 (2005) 15823–15833.
[22] G. Klocek, T. Schulthess, Y. Shai, J. Seelig, Thermodynamics of melittin binding to lipid bilayers. Aggregation and pore formation, Biochemistry 48 (2009) 2586–2596.
[23] S. Ohki, E. Marcus, D.K. Sukumaran, K. Arnold, Interaction of melittin with lipid membranes, Biochim. Biophys. Acta 1194 (1994) 223–232.
[24] T. Benachir, M. Lafleur, Study of vesicle leakage induced by melittin, Biochim. Biophys. Acta 1235 (1995) 452–460.
[25] C.E. Dempsey, The actions of melittin on membranes, Biochim. Biophys. Acta 1031 (1990) 143–161.
[26] Z. Oren, Y. Shai, Selective lysis of bacteria but not mammalian cells by diastereomers of melittin: structure–function study, Biochemistry 36 (1997) 1826–1835.
[27] H.D. Herce, A.E. Garcia, Molecular dynamics simulations suggest a mechanism for translocation of the HIV-1 TAT peptide across lipid membranes, Proc. Natl. Acad. Sci. USA 104 (2007) 20805–20810.
[28] H.D. Herce, A.E. Garcia, J. Litt, R.S. Kane, P. Martin, N. Enrique, A. Rebolledo, V. Milesi, Arginine-rich peptides destabilize the plasma membrane, consistent with a pore formation translocation mechanism of cell-penetrating peptides, Biophys. J. 97 (2009) 1917–1925.
[29] V. Tiriveedhi, P. Butko, A fluorescence spectroscopy study on the interactions of the Tat-PTD peptide with model lipid membranes, Biochemistry 46 (2007) 3888–3895.
[30] A. Ziegler, X.L. Blatter, A. Seelig, J. Seelig, Protein transduction domains of HIV-1 and SIV TAT interact with charged lipid vesicles. Binding mechanism and thermodynamic analysis, Biochemistry 42 (2003) 9185–9194.
[31] H. Yezid, K. Konate, S. Debaisieux, A. Bonhoure, B. Beaumelle, Mechanism for HIV-1 Tat insertion into the endosome membrane, J. Biol. Chem. 284 (2009) 22736–22746.
[32] D. Derse, M. Carvalho, R. Carroll, B.M. Peterlin, A minimal lentivirus Tat, J. Virol. 65 (1991) 7012–7015.

[33] H.K. Avraham, S. Jiang, T.H. Lee, O. Prakash, S. Avraham, HIV-1 Tat-mediated effects on focal adhesion assembly and permeability in brain microvascular endothelial cells, J. Immunol. 173 (2004) 6228–6233.
[34] M.E. Garber, P. Wei, V.N. Kewal Ramani, T.P. Mayall, C.H. Herrmann, A.P. Rice, D.R. Littmann, K.A. Jones, The interaction between HIV-1 Tat and human cyclin T1 requires zinc and a critical cysteine residue that is not conserved in the murine cyc T1 protein, Genes Dev. 12 (1998) 3512–3527.
[35] A.C. Vendel, K.J. Lumb, Molecular recognition of the human coactivator CBP by the HIV-1 transcriptional activator Tat, Biochemistry 42 (2003) 910–916.
[36] S. Shojania, J.D. O'Neil, HIV-1 Tat is a natively unfolded protein, J. Biol. Chem. 281 (2006) 8347–8356.
[37] J.M. Bigalke, N. Czudnochowski, V. F., K. Vogel-Bachmayr, K. Anand, M. Geyer, Formation of Tat-TAR containing ribonucleoprotein complexes for biochemical and structural analyses, Methods 53 (2011) 78–84.
[38] A. Mishra, V.D. Gordon, L. Yang, R. Coridan, G.C.L. Wong, HIV Tat forms pores in membranes by inducing saddle-splay curvature: potential role of bidentate hydrogen bonding, Angew. Chem. Int. Ed. 47 (2008) 1–5.
[39] C. Ciobanasu, J.P. Siebrasse, U. Kubitscheck, Cell-penetrating HIV1 Tat peptides can generate pores in model membranes, Biophys. J. 99 (2010) 153–162.
[40] P.E.G. Thoren, D. Persson, E.K. Esbjörner, M. Goksör, P. Lincoln, B. Norden, Membrane binding and translocation of cell-penetrating peptides, Biochemistry 43 (2004) 3471–3489.
[41] P.E.G. Thoren, D. Persson, P. Lincoln, B. Norden, Membrane destabilizing properties of cell-penetrating peptides, Biophys. Chem. 114 (2005) 169–179.
[42] C.E. Caesar, E.K. Esbjörner, P. Lincoln, B. Norden, Membrane interactions of cell-penetrating peptides probed by tryptophan fluorescence and dichroism techniques: correlations of structure to cellular uptake, Biochemistry 45 (2006) 7682–7692.
[43] T.H. Tahirov, N.D. Babayeva, K. Varzavand, J.J. Cooper, S.C. Sedore, D.H. Price, Crystal structure of HIV-1 Tat complexed with human P-TEFb, Nature 465 (2010) 747–753.
[44] G. Schwarz, R. Zong, T. Popescu, Kinetics of melittin induced pore formation in the membrane of lipid vesicles, Biochim. Biophys. Acta 1110 (1992) 97–104.
[45] G. Schwarz, A. Arbuzova, Pore kinetics reflected in the dequenching of a lipid vesicle entrapped fluorescent dye, Biochim. Biophys. Acta 1239 (1995) 51–57.
[46] C. Ciobanasu, E. Harms, G. Tünnemann, C.M. Cardoso, U. Kubitscheck, Cell-penetrating HIV-1 Tat peptides float on model lipid bilayers, Biochemistry 48 (2009) 4728–4737.
[47] P. Curnow, H. Mellor, D.J. Stephens, M. Lorch, P.J. Booth, Translocation of the cell-penetrating Tat peptide across artificial bilayers and into living cells, Biochem. Soc. Symp. 72 (2005) 199–209.
[48] N. Umezawa, M.A. Gelman, M.C. Haigis, R.T. Raines, S.H. Gellman, Translocation of a beta-peptide across cell membranes, J. Am. Chem. Soc. 124 (2002) 368–369.
[49] S.D. Krämer, H. Wunderli-Allenspach, No entry for Tat (44–57) into liposomes and intact MDCK cells: novel approach to study membrane permeation of cell-penetrating peptides, Biochim. Biophys. Acta 1609 (2003) 161–169.
[50] P. Bayer, M. Kraft, A. Ejchart, M. Westendorp, R. Frank, P. Rösch, Structural studies of HIV-1 Tat protein, J. Mol. Biol. 247 (1995) 529–535.
[51] K. Anand, A. Schulte, K. Vogel-Bachmayr, K. Scheffzek, M. Geyer, Structural insights into the cyclin T1-Tat-TAR RNA transcription activation complex from EIAV, Nat. Struct. Mol. Biol. 15 (2008) 1287–1292.
[52] J.D. Puglisi, S. Chen, S. Blanchard, R. Frank, Solution structure of a bovine immunodeficiency virus Tat-TAR peptide-RNA complex, Science 270 (1995) 1200–1203.
[53] X. Ye, R.A. Kumar, D.J. Patel, Molecular recognition on the bovine immunodeficiency virus Tat peptide-TAR RNA complex, Chem. Biol. 2 (1995) 827–840.
[54] G. Tosi, R. Meazza, A. de Lerma Barbaro, A. D'Agostino, S. Mazza, G. Corradin, A. Albini, D.M. Noonan, S. Ferrini, R.S. Accolla, Highly stable oligomerization forms of HIV-1 Tat detected by monoclonal antibodies and requirement of monomeric forms for the transactivating function on the HIV-1 LTR, Eur. J. Immunol. 30 (2000) 1120–1126.